CHAPTER II
THEORETICAL BACKGROUND AND LITERATURE REVIEW

2.1 Compliant Electrode

Dielectric electroactive polymers (DEAPs) have been developed to be used in many areas such as robot manipulators, actuators, sensors, and in combination with drug delivery systems (Arora *et al.*, 2007).The electrodes made of dielectric elastomer actuators, located on the actuator surface, are required to be conductive, soft, and can sustain large deformations while remaining conductivity, and they must be able to perform for several of cycles (Kim *et al.*, 2012).

Compliant electrodes are needed in a wide range of applications. Certainly, the booming field of soft and deformable electronics also relies on flexible interconnects that can sustain stretching and/or bending under electric field as shown in Figure 2.1.

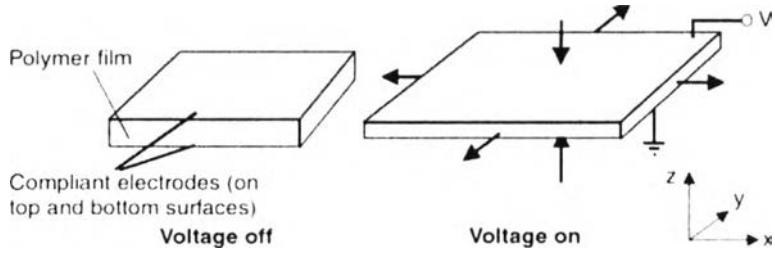

Figure 2.1 Application of compliant electrode, it provides current to dielectric actuator then material is squeezed out (Pelrine *et al.*, 2000).

Thus, it is required that the compliant electrode should be of high conductivity and elasticity. Developed elastic conductors containing conductive fillers can enhance the electrical conductivity (Someya *et al.*, 2009, Rosset *et al.*, 2013).

The performance of a dielectric elastomers (DE) actuator depends in part on the electrode material used. Electrode materials using in this application should ideally satisfy the following criteria (Schlaak *et al.*, 2005):

- Highly compliant (i.e. Young's modulus <100 MPa (Delille *et al.*, 2006);
- Low electric resistance under large strain;
- High surface density under large strain;
- Thin in thickness in comparison to the dielectric layer;
- Ability to be patterned with high resolution;
- Good adhesion to the dielectric layer;
- Conducive to typical DE actuator manufacturing processes (layering, rolling);
- Longevity

The frequency response of the actuator is dependent on charging time and consequently the resistance of the electrodes (Schlaak *et al.*, 2005). However, in reality, the speed of response is determined by the mechanical reaction time of the highly viscous material (Delille *et al.*, 2006).

Table 2.1 Comparisons of compliant electrode properties

Materials	Thermal conductivity (W/mK)	Conductivity (S/cm)	Elongation (%)	Young's modulus (MPa)	Tensile strength (MPa)	Strain (%)	Hardness (Shore A)
EG/NBR nanocompo sites (Yang *et al.*, 2007)	0.30	0.3	110	-	11.8	-	-
SWNT/vin ylidene fluoride-hexafluoro-propylene composite (Sekitani *et al.*, 2008)	-	57	-	-	-	134	-

Table 2.1 Comparisons of compliant electrode properties (cont.)

Materials	Thermal conductivity (W/mK)	Conductivity (S/cm)	Elongation (%)	Young's modulus (MPa)	Tensile strength (MPa)	Strain (%)	Hardness (Shore A)
Graphite/ PDMS composite (Kujawski *et al.*, 2010)	-	0.4	-	1.4	-	-	-
MWNT/PU composite (Shin *et al.*, 2010)	-	0.5	-	-	-	-	-
GNP/silicone composites (Raza *et al.*, 2011)	1.909	3.6×10^{-3}	-	-	-	-	60.8
SWCNT/silicone rubber composites (Kim *et al.*, 2012)	-	63	-	-	1.84	-	-
MWNT/ PDMS composites (Lee *et al.*, 2012)	-	3×10^{-3}	-	2.22	-	-	-
CNT and CB/silicone rubber composite (Witt *et al.*, 2013)	-	8.0×10^{-6}	-	-	-	789.7	-

Yang et al. (2007) studied high performance elastomeric nanocomposites with improved mechanical properties and functional properties. And they found that nanocomposites exhibit intercalation of graphite in the nitrile-butadiene rubber (NBR) matrix. Mechanical and dynamic-mechanical tests demonstrate that the NBR/graphite nanocomposites possess greatly increased elastic modulus and tensile strength (11.8 MPa), and desirably strong interfaces. These NBR/graphite

nanocomposites possess significantly improved wear resistance and gas barrier properties, and superior electrical (0.3 S/cm) /thermal conductivity (0.3 W/mK) (Yang *et al.*, 2007).

Sekitani et al. (2008) studied elastic conductors by using an ionic liquid of 1-butyl-3-methyl-imidazoliumbis (trifluoromethanesulfonyl)imide. They uniformly dispersed single-walled carbon nanotubes (SWNTs) as chemically stable dopants in a vinylidenefluoridehexafluoropropylene copolymer matrix to form a composite film. They found that the SWNT content could be increased up to 20 weight percent without reducing the mechanical flexibility or softness of the copolymer. The SWNT composite film was coated with dimethylsiloxane–based rubber, which exhibited a conductivity of 57 S/m and a stretch ability of 134%. Furthermore, the elastic conductor was integrated with printed organic transistors to fabricate a rubber-like active matrix with an effective area of 20 x 20 centimeters square. The active matrix sheet could be uniaxially and biaxially stretched by 70% without mechanical or electrical damage. The elastic conductor allowed the construction of electronic integrated circuits, which could be mounted anywhere, including arbitrary curved surfaces and movable parts, such as the joints of a robot's arm (Sekitani *et al.*, 2008).

Kujawski et al. (2010) studied the compliant electrode material realized by blending an insulating polydimethylsiloxane (PDMS) elastomer with a conductive exfoliated graphite filler. These materials exhibited a low percolation threshold: above 3 wt% loading, they became conductive, with conductivities reaching as high as 0.4 S/cm. This electrode remained elastomeric upon loading up to 25 wt%, having a Young's modulus of 1.44 MPa. It was claimed that this modulus was the lowest reported for loaded elastomers above the percolation threshold. It was also capable of undergoing large deformations (ultimate strains as large as 250% after extended cycling), and it was durable (5 wt% samples were capable of 106 cycles to 30% strain without failure) (Kujawski *et al.*, 2010).

Shin et al. (2010) developed rubberlike transistor-active matrices that can be stretched biaxially by 70%. For electrical measurements, prepared sheets were cut into about $20\times3\times0.25$ mm^3 strips. The overall electrical conductivity of the strips was 10–20 S/m with the conductivity of the forest/ PU layer being about 50-100 S/m. The latter is close to the value expected if the pristine MWNT forests grown on Si wafers

retained their electrical conductivity upon infiltration. This conductivity is 1–2 orders of magnitude. The commercially available carbon-filled rubbers (Stockwell Elastomerics, Inc., Philadelphia, USA) typically have the conductivity 2–20 S/m, tensile strength 2–6MPa, and strain at break 100%–275%. These values are markedly lower than the corresponding values for the prepared forest/PU composites. The elasticity of the prepared forest/PU composite was evaluated using tensile stress vs. strain measurements. The initial Young's modulus and final mechanical strength of this composite calculated from engineering stress– strain curves were about 19.4MPa and 10.1MPa, respectively. These values of Young's modulus and strength were 148% and 38%, respectively (Shin *et al.*, 2010).

Raza et al. (2011) studied thermally conducting and highly compliant composites by dispersing graphite nanoplatelets (GNPs) into a silicone matrix by mechanical mixing. X-ray diffraction (XRD) indicates that the average thickness of the GNPs decreased from 60 to 35 nm during mechanical mixing. XRD-texture analysis demonstrated that GNP/silicone composites at 8 wt% GNPs have a higher degree of basal plane alignment than at 20 wt%. The thermal conductivity of the 20 wt% composites reached 1.909 W/m.K. The percolation threshold for electrical conductivity of the composites was at 15 wt%. The compressive modulus of the composite increased to twice that of silicone at 20 wt%. The corresponding strength decreased by a factor of two compared to silicone and this can be attributed to the weak bonding at the GNP-silicone interface (Raza *et al.*, 2011).

Kim et al. (2012) prepared highly stretchable and conductive silicone rubber composites by adding gels composed of SWCNTs and animidazolium-based IL. These composites were stretched to three times length and they still retained their high conductivity (18 S/cm) even after 20^{th} stretch/release/stretch cycle. Thus, these materials could be useful as stretchable conductors that retained a constant conductivity when a high tensile strain up to 200% was applied (Kim *et al.*, 2012).

Lee et al. (2012) developed stretchable, elastomeric composite conductor made of multi-walled carbon nanotubes (MWNTs) with polydimethylsiloxane (PDMS) by simple mixing. Electrical percolation threshold, amount of filler at which a sharp decrease of resistance occurs, has been determined to be 0.6 wt% of MWNTs. The percolation threshold composition has also been confirmed from

swelling experiments of the composite; the equilibrium swelling ratio slightly increases up to 0.6 wt%, then decreases at higher amount of filler MWNTs. Upon cyclic stretching/release of the composite, a fully reversible electrical behavior has been observed for composites having filler content below the percolation threshold value. On the other hand, hysteretic behavior was observed for higher filler amount than the threshold value, due to rearrangement of percolative paths upon the first cycle of stretching/release. Finally, mechanical moduli of the composites have been measured and compared by buckling and microtensile test. The buckling-based measurement has led to systematically higher (20%) value of moduli than microtensile measurement, due to the internal microstructure of the composite. The elastic conductor may help the implementation of various stretchable electronic devices (Lee *et al.*, 2012).

Witt et al. (2013) prepared conductive silicone rubber (SR) composite, filled with both carbon nanotubes (CNTs) and carbon black (CB) was prepared by a simple ball milling method. Because of the good dispersion and synergistic effects of CNT and CB, the SR composite (SR with 2.5 phr CB and 1.0 phr CNT hybrid fillers) showed improvement in mechanical properties such as tensile strength and strain to failure. As well, due to the assembly of conductive pathways generated by the CNT and CB, the nanocomposite became highly conductive at a comparatively low concentration, with high sensitivity for tensile and compressive stress. Long-term measurement of properties shows that the SR composite maintains the excellent electrical properties under different strain histories. These outstanding properties show that the SR composite has potential applications in tensile and pressure sensors (Witt *et al.*, 2013).

2.2 Graphene

Graphene is the most notable and recent examples of materials that are organic conductors. It has been long tempted to extend the use of the field effect to metals, to develop all metallic transistors that could be scaled down to much smaller sizes and would consume less energy and operate at higher frequencies than traditional semiconducting devices (Liao *et al.*, 2010). Nevertheless, this would

require atomically thin metal films, because the electric field is screened at extremely short distances (<1 nm) and bulk carrier concentrations in metals are large compared to the surface charge that can be induced by the field effect as shown in Figure 2.3.

Krishnamoorthy et al. (2013) studied a facile sonochemical route for the synthesis of graphene nanosheets via reduction of graphene oxide (GO) has been reported. The synthesized graphene sheets are characterized using UV–vis spectra, Fourier transform infra-red (FT-IR) spectra, transmission electron microscope, X-ray photoelectron spectra (XPS) and Raman spectroscopic techniques. The UV–vis spectroscopy results showed that the absorption peak was red shifted due to the reduction of GO into graphene. FT-IR and XPS spectra revealed the removal of oxygenated functional groups in graphene after the reduction process. Raman spectra confirmed the restoration of new sp^2 carbon domains in graphene sheets after the reduction. The sonochemical approach for the synthesis of graphene nanosheets is relatively fast, cost-effective and efficient as compared to other methods. (Krishnamoorthy *et al.*, 2013).

Graphene can be produced by seven different methods, including the micromechanical exfoliation of graphite (Novoselov *et al.*, 2004), the epitaxial growth on the electrically insulating surfaces (Berger *et al.*, 2004), the chemical vapor deposition method of hydrocarbons on the transition metal substrates (Lee *et al.*, 2010), the electric arc discharge (Lee *et al.*, 2010), the direct sonication (Mustafa *et al.*, 2009), the un-zipping carbon nanotubes (Kosynkin, 2009), and the solution-based graphene oxide (GO) of chemical reduction (Mustafa *et al.*, 2009). However, the chemical reduction method has received the most attention as it is considered as the best possible route for industrial production due to its simple procedure and low cost. Typically, graphene is prepared from the oxidation of graphite powder by a modified Hummers method and a subsequent reduction process (Perera *et al.*, 2012).

Fernández-Merino et al. (2010) studied the work focusing on the chemical reduction process of GO which was considered as an effective method to produce graphene on a large-scale at low cost. Hydrazine hydrate was widely considered to be the most efficient reduction agent to date. They also left oxygen atoms remaining on the graphene and could introduce additional functional groups during the

chemical reduction. Recently, different reducing agents had been reported to substitute hydrazine hydrate (Fernández-Merino *et al.*, 2010).

Novoselov et al. (2004) reported the chemical reduction of GO using vitamin C as an ideal substitute for hydrazine. However, expensive vitamin C and long experimental time limited a practical application (Novoselov *et al.*, 2004).

Antonio Castro Neto (2006) was able to prepared graphitic sheets of thicknesses down to a few atomic layers (including single-layer graphene) in order to fabricate devices and to study their electronic properties. Despite being atomically thin, the films remained of high quality, and the 2D electronic transport was ballistic at sub-micrometer distances. No other film of similar thickness was known to be even poorly metallic or continuous under ambient conditions. Using few-layer graphite (FLG), they demonstrated with a metallic field-effect transistor in which the conducting channel could be switched between 2D electron and hole gases by changing the gate voltage.

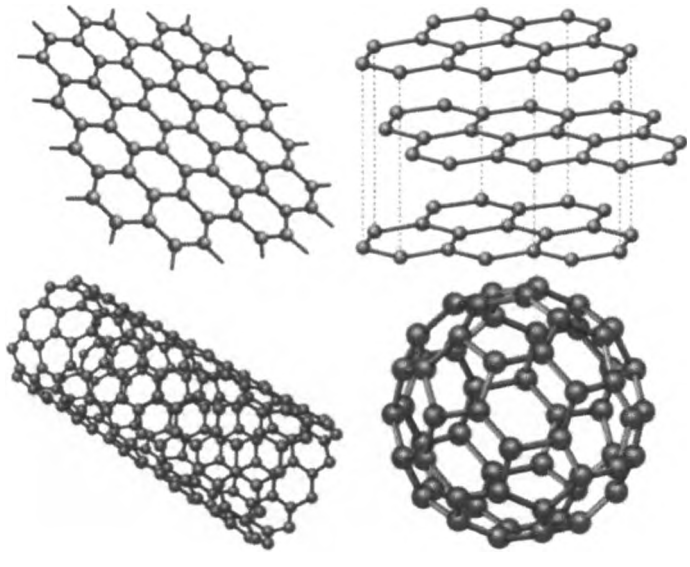

Figure 2.2 Graphene (top left) is a honeycomb lattice of carbon atoms. Graphite (top right) can be viewed as a stack of graphene layers. Carbon nanotubes are rolled-up cylinders of graphene (bottom left). Fullerenes (C60) are molecules consisting of a wrapped graphene through the introduction of pentagons on the hexagonal lattice (Antonio Castro Neto, 2006).

Wang et al.(2007) studied graphene, as a nanofiller, to be preferred over other conventional nanofillers (Na-MMT, LDH, CNT, CNF, EG, etc.) owing to high surface area, aspect ratio, tensile strength, thermal conductivity and electrical conductivity, EMI shielding ability, flexibility, transparency, and low CTE (Wang *et al.*, 2007).

Table 2.2 Comparative chart on the mechanical, thermal and electrical properties of graphene with CNT, steel, plastic, rubber, and fiber

Materials	Tensile strength	Thermal conductivity (W/mk) at room temperature	Electrical conductivity (S/m)
Graphene	130±10 GPa	$(4.84\pm0.44)\times10^3$ - $(5.30\pm0.48)\times10^3$	7200
CNT	60–150 GPa	3500	3000–4000
Nano sized steel	1769 MPa	5–6	1.35×10^6
Plastic (HDPE)	18–20 MPa	0.46–0.52	Insulator
Rubber (natural rubber)	20–30 MPa	0.13–0.142	Insulator
Fiber (Kevlar)	3620 MPa	0.04	Insulator

Stankovich et al.(2006) reported as in Table 2.1 a comparative chart on the mechanical, thermal and electrical properties of graphene with CNT, steel, plastic, rubber and fiber. The tensile strength of graphene is similar or slightly higher than CNT, but much higher than steel, Kevlar, HDPE, and natural rubber. The thermal conductivity of graphene is higher than all these materials. The electrical conductivity of graphene is also higher than these materials except for steel.

McAllister et al. (2007), Stankovich et al. (2006), and Becerril et al. (2008) reported the superior properties of graphene compared to polymers and through polymer/graphene nanocomposites. Polymer/graphene nanocomposites showed superior mechanical, thermal, gas barrier, electrical and flame retardant properties when compared to the neat polymer (Stankovich, 2006). It was also reported that the

improvement in mechanical and electrical properties of graphene based polymer nanocomposites were much better in comparison to that of clay or other carbon filler-based polymer nanocomposites. Although CNT showed comparable mechanical properties compared to graphene, graphene was better nanofiller than CNT in certain aspects, such as thermal and electrical conductivity. However, the improvement in the physico-chemical properties of the nanocomposites depends on the distribution of graphene layers in the polymer matrix as well as interfacial bonding between the graphene layers and polymer matrix. Interfacial bonding between graphene and the host polymer dictates the final properties of the graphene enforcing polymer nanocomposite. Pristine graphene was not compatible with organic polymers and did not form homogeneous composites. In contrast, graphene oxide sheets were heavily oxygenated graphene (bearing hydroxyl, epoxide, diols, ketones and carboxyls functional groups) that could alter the van der Waals interactions significantly and be more compatible with organic polymers (McAllister *et al.*, 2007, Becerril *et al.*, 2008). There were also some additional carbonyl and carboxyl groups located at the edge of the sheets, which made graphene oxide sheets strongly hydrophilic, allowing them to readily swollen and dispersed in water (Szabó *et al.*, 2005, Nethravathi *et al.*, 2008). For this reason, GO has attracted considerable attention as a nanofiller for polymer nanocomposites. However, GO sheets could only be dispersed in aqueous media, which were incompatible with most organic polymers. In addition, unlike graphene, graphene oxide was electrically insulating, which makes it unsuitable for the synthesis of conducting nanocomposites. The surface modification of graphene was an essential step for obtaining a molecular level dispersion of individual graphene in a polymer matrix. The electrical conductivity of the resulting nanocomposites can be increased by the chemical reduction of GO, presumably by restoring the graphitic network of sp^2 bonds (Stankovich, 2006).

Pang et al.(2010) studied a graphene nanosheet/ultra-high molecular weight polyethylene composite with a segregated structure which had been fabricated using water/ethanol solvent-assisted dispersion and hot compression at 200 °C. A percolation threshold as low as 0.070 vol.% had been achieved because of the formation of a two dimensional conductive network (Pang *et al.*, 2010).

Zhou et al. (2011) used sodium hydrosulfite in reducing graphite oxide. The preparation of poly (vinyl alcohol) (PVA)/graphene nanocomposites was realized using two simple steps: the synthesis of PVA/graphite oxide (GO) nanocomposites film and the immersion of such a film in the reducing agent aqueous solution. This method prohibited the agglomeration of GO during the direct reduction in PVA/GO aqueous solution and opened a new way to scale up the production of graphene nanocomposites using a simple reducing agent. A 40% increase in tensile strength and 70% improvement in elongation at break were obtained with only the addition of 0.7 wt% of reduced graphite oxide. Furthermore, the highest conductivity achieved was 8.9×10^{-3} S/m for the composites containing 3 wt% reduced graphene oxide (rGO), and the conductivity achieved was comparable to those achieved with hydrazine. In addition, rGO could largely increase the contact angle of PVA matrix by around 10 degree due to its hydrophobic nature (Zhou *et al.*, 2011).

Kujawski et al. (2010) fabricated compliant electrode material as realized by blending an insulating polydimethylsiloxane (PDMS) elastomer with conductive exfoliated graphite filler, as produced by a microwave irradiation. The conductivity and stiffness of the electrodes were determined as functions of filler concentration. These materials exhibited a low percolation threshold: above 3 wt% loading they became conductive, with conductivity reaching as high as 0.4 S/cm. They remained elastomeric upon loading up to 25 wt%, having a Young's modulus of only 1.4 MPa. This modulus was the lowest reported for loaded elastomers above the percolation threshold. It was also capable of undergoing large deformations (ultimate strains as large as 250% after extended cycling), and it was durable (5 wt% samples were capable of 106 cycles to 30% strain without failure). The performance of these electrodes was comparable to that of PDMS loaded with carbon nanotubes, but the exfoliated graphite material can be produced at a fraction of the cost (Kujawski *et al.*, 2010).

Kalaitzidou et al. (2007) studied nanocomposites made of polypropylene reinforced with exfoliated graphite nanoplatelets (xGnP) as fabricated by melt mixing, in a polymer solution and coating. Coating was a new compounding method proposed in this work, where xGnP and PP powders were premixed in isopropyl alcohol using sonication to disperse the xGnP by coating individual PP powder

particles. It was found that the coating method was more effective than the polymer solution method widely used, in terms of lowering the percolation threshold of thermoplastic nanocomposites and enhancing the probability that the large platelet morphology of xGnP could be preserved in the final composite. The conductivity of xGnP/PP nanocomposites made by the premixing compounding method was as high as 10^{-4} S/cm at a loading of 3 vol. %, indicating that the percolation threshold which could be achieved by this method was much lower than the others. For both xGnP loadings used, 3 and 5 vol. %, the proposed coating method resulted in conductivity higher than the conductivity of the polymer solution processed sample with a lower percolation threshold 0.1 vol. %, for the samples made by coating and compression molding. Composites with similar compositions made by melt mixing and injection molding had a percolation threshold of 7 vol. %. Additionally, advantages of this method are that the experimental set up was very simple, no solvents were used, there was no need for high temperatures, and the non-solvent can be easily recycled making the method to be practical, safe, cost and time effective, and environmentally friendly (Kalaitzidou *et al.*, 2007).

Hernández et al. (2012) studied natural rubber (NR) and functionalized graphene sheets (FGSs) nanocomposites as prepared by a conventional two-roll mill mixing. The morphology and structure of the FGS were characterized confirming the successful exfoliation of the FGS. The strong rubber-to-filler interactions accelerated the cross-linking reaction, increased the electrical conductivity at higher nanofiller concentrations, suggesting a percolation threshold between 0.1–0.5 phr causing an important enhancement on the mechanical behavior of the NR nanocomposites. The nanofiller did not affect the molecular dynamics of NR, while the presence of vulcanizing additives slow downed the segmental motions and decreased slightly the timescale of the global chain dynamics in NR/FGS nanocomposites (Hernández *et al.*, 2012).

Table 2.3 Physical properties of different carbon materials (Ma *et al.*, 2010)

Properties	Graphite	Diamond	Fullerene	SWCNT	MWCNT
Specific gravity (g/cm^3)	1.9–2.3	3.5	1.7	0.8	1.8
Electrical conductivity (S/cm)	4000	10^{-2}–10^{-15}	10^{-5}	10^{2}–10^{6}	10^{3}–10^{5}
Electron mobility ($cm^2/(V\ s)$)	$2.0 - 10^4$	1800	0.5–6	10^5	10^4–10^5
Thermal conductivity (W/(m K))	298	900–2320	0.4	6000	2000
Coefficient of thermal expansion (K^{-1})	2.9×10^{-5}	3×10^{-6}	6.2×10^{-5}	Negligible	Negligible
Thermal stability in air (°C)	450–650	<600	~600	>600	>600

2.3 Natural Rubber

Natural rubber (NR) is a local tree in Brazil and Guianas. First discovered by the ancient Olmec, Maya and Aztec, the latex sap from the rubber tree was once used to make rubber balls, to waterproof clothes, and even to form homemade shoes(Manmoun, 2013). Today, the latex sap from the rubber tree is still used in the modern processing of rubber and is often a substantial source of income for indigenous populations. At present, most of the world's rubber comes from agricultural estate in Indonesia, Thailand and Malaysia. Rubber tree common names are caoutchouc tree, hevea, para rubber tree, rubber, rubber wood, and yang para. Scientific name is *Heveabrasiliensis* (A. Juss) Muell. Arg and molecular chemical structure of natural rubber is cis-1,4-polyisoprene as shown in Figure 2.3. (Piya-areetham *et al.*, 2013).

Fresh latex from the rubber tree contains 28–35 wt% dry rubber content (Khamput *et al.*, 2011). After collection, the fresh latex is stabilized with NH_3 and transported from the plantation to an industry where it undergoes continuous centrifugation to produce concentrated NR latex, containing ~60 wt% dry rubber content. For long-term preservation and transport the latex to the factories, the latex is concentrated for saving the transportation cost, the NH_3 content is usually raised to 0.6–0.7 wt%; this is referred to as high-ammonia preserved concentrated latex.

Medium-ammonia preserved concentrated latex contains 0.4–0.5 wt% NH_3. Low-ammonia preserved concentrated latex contains only 0.2–0.3 wt% NH_3. Tetramethylthiuram disulfide (TMTD) is used as a bactericide (Khamput *et al.*, 2011).

Table 2.4 The composition and functions of components in NR latex (Rojruthai, 2012)

Component	Concentration (wt%)	Function of component
Rubber hydrocarbon	35	Main component of NR
Proteins	1.4	Enfold rubber particle
Lipids	1.6	Serve as covering on the surface of the rubber particle and fix proteins cover on rubber particle.
Carbohydrate	1.6	When it was digested by bacteria, it will generate small acid to reduce stability of
Inorganic	0.5	latex.
constituents	0.4	Prooxidants
Other	58.5	β-carotene causes yellow color and
Water	the rest	polyphenol oxidase oxidation and storage hardeningmedium of latex

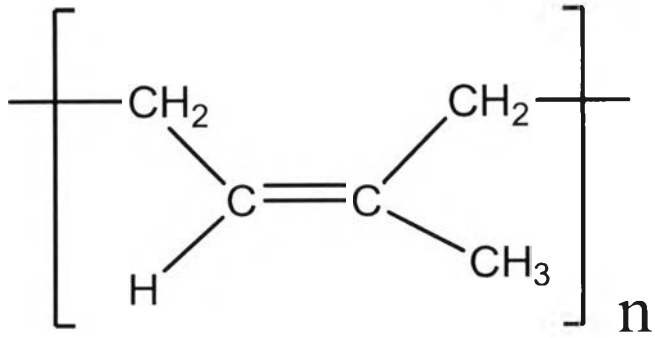

Figure 2.3 Molecular chemical structure of natural rubber, cis-1,4-polyisoprene (Deiters *et al.*, 2006).

Yigit et al. (1996) studied an electrochemical synthesis of conducting polymer polythiophene. Synthetic and natural rubbers were used as the insulating polymer matrices. Fourier transform infrared spectrometer (FT-IR), differential scanning calorimeter (DSC), scanning electron microscopy (SEM) and mass spectrometry (MS) were utilized to characterize the composite blends. The conductivity measurements were done by using a standard four-probe technique. The above-mentioned methods showed that the resultant composites had different properties relative to those of polythiophene due to the interaction of the rubbers with the electrochemical polymerization of thiophene, whereas the same argument was not valid for the polypyrrole synthesis via the same procedure (Yigit *et al.*, 1996).

Table 2.5 Conductivities of NR-PTh films (Yigit *et al.*, 1996)

% PTh	Conductivity (S/cm)
80	3.0×10^{-1}
85	3.5×10^{-1}
90	3.2×10^{-1}
95	3.7×10^{-1}

The measured conductivities of NR-PTh films according to the weight percent of the PTh in composite blends are given in Table 2.4. The high percentages of PTh in the composites were due to losses in rubber content during the thiophene polymerization. This method did not allow us to obtain high rubber content composite films (Yigit *et al.*, 1996).

Hernández et al. (2012) studied a natural rubber (NR) and functionalized graphene sheets (FGSs) nanocomposites which were prepared by a conventional two-roll mill mixing. The morphology and structure of the FGS were characterized confirming the successful exfoliation of the FGS. The strong rubber-to-filler interactions accelerated the cross-linking reaction, increased the electrical conductivity at the higher nanofiller concentrations, suggesting a percolation threshold between 0.1– 0.5 phr, and caused an important enhancement on the mechanical behavior of the NR nanocomposites. The nanofiller did not affect the molecular dynamics of NR, while the presence of vulcanizing additives slow downed the segmental motions and decreased slightly the timescale of the global chain dynamics in NR/FGS nanocomposites (Hernández *et al.*, 2012).

Matos et al.(2012) described the synthesis, characterization, and studied properties of novel multifunctional composite materials obtained by natural rubber latex and a special kind of multi-walled carbon nanotubes (CNTs), in which the cavities were filled by magnetic species. To prepare stable aqueous dispersions of CNTs, two approaches had been employed, based on a mixture of the surfactant sodium dodecyl sulfate or a previous treatment with a mixture of acid solutions. Several samples had been prepared containing different amounts of CNTs from 0.01 to 10 wt%. The occurrence of networks of CNTs in the polymeric matrices provided significant effects of the CNTs on the electrical, mechanical, chemical and thermal properties and the solvent sorption. Additionally, because of the species encapsulated in CNTs, the composites exhibited magnetic behavior, as confirmed by the magnetic force microscopy. This approach resulted in a novel multifunctional material with a great potential for further applications (Matos *et al.*, 2012).

Kueseng et al. (2013) studied CNTs/NR master batches prepared by pre-dispersing and conventional methods were mixed with NBR for preparing CNTs-filled 50/50 NR/NBR blends. The amount of CNTs in the blends was varied from 0

to 6 phr. At a given CNTs loading, the hardness, modulus, tensile strength and tear strength of the blends containing the masterbatches prepared by the pre-dispersing method were significantly higher than those prepared by the conventional method. This was simply due to the better CNTs dispersion in the blends. Additionally, dynamic mechanical results showed that the maximum tan delta of the vulcanization containing the masterbatches prepared by the pre-dispersing method was lower than that of the corresponding conventional samples. This behavior indicated the stronger reinforcing efficiency when the masterbatch prepared by the pre-dispersing method was utilized. In addition, thermal conductivity of the blend having 4 phr of CNTs was 1.7 times higher than that of the corresponding sample prepared by the conventional method (Kueseng *et al.*, 2013).

2.4 Vulcanization of Rubber

The vulcanization is a process that transforms the thermoplastic or raw rubber into an elastic or hard ebonite-like state. This process is also known as ''crosslinking'' or ''curing'' and involves the association of macromolecules through their reactive sites.

Haque et al. (1996) studied the crosslinking or the reaction of a rubber to form a three-dimensional network. Cure of the rubber resulted in the vulcanization making it more elastic. When the NR was irradiated by high energy radiation, hydrogen atoms of the trunk chain, mainly of the methylene group proportional to double bonds, were ejected and radical sites were formed, and these radical sites were combined into C-C crosslink. The addition of NR radicals is to unsaturated C5C bond provided formation of crosslinks. However, the radiation crosslinking efficiency of NR was not high. This was believed to be due to the loose packing of NR molecules with the cis-structure and the presence of methyl group (Haque *et al.*, 1996).

Atieh et al. (2010) studied an ultraviolet (UV) radiation curing, a widely established area of industrial importance and academic interest. This was due to the combined attributes of rapid, energy efficient curing at ambient temperature on exposure to radiation and the possibility of achieving formulation free of volatile

organic components. Because of its distinct advantages, the photo-curing technology had found a growing number of applications, mainly in coating industry, graphic arts, microelectronics, wood finishes, photo resists, electronics/electrical, decorative applications, converting/packaging, dental restorations, flooring, and adhesives (Atieh *et al.*, 2010).

Wang et al. (1995) reported that UV curing was similar to polymerization reactions which involved free radical, cationic or anionic mechanisms depending on the functional group or unsaturated bond of the prepolymer and with initiators or catalyst. A methodology had been established for systematically evaluating polymer films produced by UV curing. Cast films of 1,3-bis[(p-acryloxymethyl)phenethyl] tetramethyldisiloxane (I) and norborenylpolydimethylsiloxane (II) were cured by UV irradiation. The films were evaluated from real-time FTIR studies, a non-rheologically destructive method for determining micro-viscosity, dynamic mechanical thermal analysis (DMTA), and leaching and swelling studies. Real-time FTIR indicated that while conversion from a prepolymer to a network was complete for (II), conversion was only 80% for (I) with 0.05% benzoin methyl ether (BME), an initiator, and only 60% with 0.5% BME. Results of DMTA showed the glass transition temperatures (T_g values) of the films to had an inverse rank order correlation with conversion. Along with micro viscosity results, this was indicative of a diffusion rate-limited curing reaction. Results of leaching and swelling demonstrated greater rates and extents of leaching and swelling from films prepared with a lower concentration of initiator (0.05% BME). These observations were in good agreement with the results from the micro viscosity and DMTA studied which showed larger free volumes and lower T_g values as well as slightly lower crosslinking densities in films prepared with a lesser amount of initiator. The methods presented in this work had been shown to be useful in quantifying the reaction of this new class of film formers and in identifying the mechanisms of film formation (Wang *et al.*, 1995).

Keller et al. (2004) studied the photo-curable composite resin made of four major components: an acrylic monomer, an acrylate functionalized oligomer, a photoinitiator and the mineral filler. Nanocomposite materials made of silicate platelets dispersed in a crosslinked polymer have been produced by photo-initiated

polymerization of a multifunctional acrylic resin containing organophilic clay. Exfoliation of the silicate nanoparticles was demonstrated by X-ray diffraction spectroscopy and by transmission electron microscopy. Under intense illumination, the solvent-free hybrid formulation was transformed within seconds into a hard and tough material at ambient temperature. An acrylate end-capped polyurethane, PUA (Ebecryl284 or Ebecryl 8402 from UCB Chemicals), was used as telechelic oligomer (M=1200 g). Hexanedioldiacrylate (HDDA from UCB Chemicals) was used as reactive diluents at a weight concentration of 27% to reduce the formulation viscosity. A combination of two photoinitiators, a hydroxyphenylketone (2 wt% Darocur 1173 from Ciba SC) and anacylphosphine oxide (1 wt% Irgacure 819 from CibaSC), was chosen to achieve both surface and deep through area, respectively. The fast photo-bleaching of the strongly absorbing acylphosphine oxide photoinitiator made the incident radiation penetrated progressively deeper into the sample, thus promoting a frontal polymerization process (Keller *et al.*, 2004).

Yuan et al.(2012) studied the primary UV curable resin formulation utilized which was a 7:2:1 mixture of EB270: HDDA: TPGDA. The above synthesized LDH-SA was added into the resin with the respective concentrations of 1, 3, and 5 wt%, and stirred for 48 h to achieve the complete dispersion. After toluene was removed under vacuum, a radical fragmental photoinitiator, Runtecure 1104, (3 wt%) was added and stirred for 2 h. All the operations were performed in dark to prevent any unexpected polymerization. The pure organic formulation as referenced was obtained by EB270: HDDA: TPGDA (7:2:1) with 3 wt% Runtecure 1104. The above obtained UV curable blends were exposed to a medium pressure mercury lamp (1 kW, Fusion UV systems, USA) with the band conveyer speed of 2.2 m min^{-1} at the incident light intensity of 30 mW cm^{-2} on the samples. Moreover, the UV cured polymer/LDH nanocomposites containing the LDH-SA with the respective concentrations of 1, 3, and 5 wt% were named as LS1, LS3, and LS5, respectively (Yuan *et al.*, 2012)

2.5 Polymer/Carbon Filler Composite

A relatively new approach to incorporate carbon fillers into a polymer matrix is based on the use of latex technology. Latex is a colloidal dispersion of discrete polymer particles, usually in an aqueous medium. By using this technology, it is possible to disperse carbon base materials in polymers. Contrary to the in situ polymerization system, the addition of carbon fillers in this technique takes place after the polymer has been synthesized. The first step of the process consists of exfoliation or dispersion/stabilization of carbon fillers in an aqueous surfactant solution, followed by mixing the stable dispersion of surfactant- treated carbon fillers with a polymer latex. The advantages of this technique are obvious in the Toolbox for dispersing carbon fillers into polymers to get conductive nanocomposites by (Grossiord *et al.*, 2006). The solvent used for carbon fillers dispersion is water, thus the process is a safe, environmentally friendly and low-cost method. Nowadays, polymer latex is industrially produced on a large scale(Ma *et al.*, 2010).

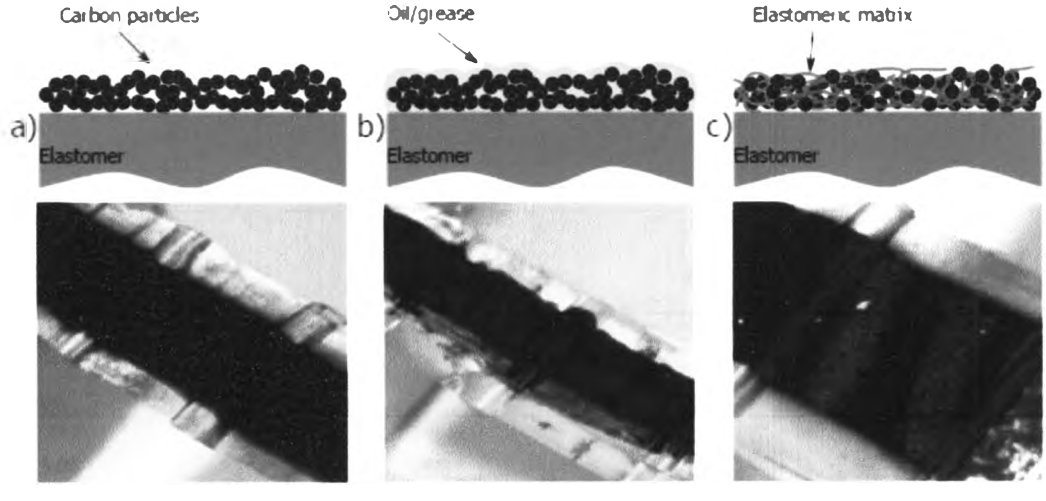

Figure 2.4 The three main types of carbon-based electrodes: a) Loose carbon powders particles directly applied on the elastomer membrane; b) Carbon grease consists of carbon particles dispersed in a viscous oil; and c) Conductive rubber consists of carbon particles dispersed into a crosslinked elastomer (Rosset *et al.*, 2013).

In the field of conductive polymer nanocomposites, researchers are usually aiming at a controlled and low percolation threshold and a satisfactory overall conductivity combined with enhanced mechanical properties. Tuning these properties is always a challenge, as many parameters are involved and play a role in the system, starting from the selection of the components (filler, polymer matrix plus optional surfactant), passing through the optimum ratio filler/matrix or filler/surfactant/matrix and finishing with one of the methods used for obtaining a good nanofiller dispersion and processing of the composite.

Tkalya et al. (2012) studied ultra-sonication of graphite for 140 min in the presence of surfactant, followed by centrifugation and filtration. This yielded transparent film with conductivity up to 1.5×10^4 S/m. Similar results were obtained for SWCNTs/water systems sonicated in the presence of SDS and spray-coated on a glass substrate. The balance between the final conductivity values and the transparency is still needed to be optimized in order to be able to apply these systems commercially in an efficient way. Probably, the presence of remaining surfactant is still an issue hindering conductivity in this case. Note that the alkyl chain length can be neither too short (the extent of increase of the hydrophobic interaction and the miscibility is not enough), nor too long (the thermal stability may be deteriorated). The conductivity of the composites was shown to reach 4 S/m in which the surfactant also proved to contribute a little. PS composite containing only a surfactant exhibited a conductivity up to 0.006 S/m (Tkalya *et al.*, 2012).

Martin-Gallego et al. (2013) studied and compared the filler percolation network of multi-walled carbon nanotubes (MWCNTs), as grown by a chemical vapor deposition and thermally reduced functionalized graphene sheets (FGSs) in an epoxy resin. The filler network was evaluated by the plate– plate rheological response of un-cured dispersions and the electrical properties of cured materials. It was found that FGS did not raise the viscosity of the system as much as MWCNT, maintaining the Newtonian behavior even at 1.5wt% FGS. MWCNT readily formed a filler network compared to FGS, as evidenced by lower electrical and rheological percolation thresholds, the presence of yield stress, and higher storage modulus of the dispersions. On the other hand, the mechanical performance of the cured FGS nanocomposites outperformed the MWCNT, with enhancements of 50% and 15% of

Young's modulus and strength, respectively. This combination of good processing properties with low viscosity and enhanced mechanical properties made FGS great candidates to develop as multifunctional polymer materials (Martin-Gallego *et al.*, 2013).

Banerjee et al. (1995) and Jing et al. (2000) found a new compounding method for exfoliated graphite–polypropylene nanocomposites with enhanced flexural properties and a lower percolation threshold. The important properties in electrical conductive composites were the electrical conductivity, reported as bulk conductivity, and the percolation threshold defined as the minimum volume content of the conductive reinforcement above which the polymer composite became electrically conductive. It was desirable for the conductive filler content to be as low as possible in order to achieve good process ability, low cost, and satisfactory mechanical performance. Both the conductivity and the percolation threshold were affected by various factors such as the volume fraction and geometric characteristics of the conductive filler (Banerjee *et al.*, 1995, Jing *et al.*, 2000), the filler orientation and spacing within the polymer matrix (Göktürk *et al.*, 1993, Fiske *et al.*, 1997) as well as the crystallinity of the matrix (Chodak *et al.*, 1999). The fabrication method and processing conditions of the composites played an important role in the percolation threshold and conductivity since they affected the orientation, dispersion, and inter particle spacing within the polymer matrix where they might alter the filler's aspect ratio, or enhance the interactions between filler and matrix, and change the matrix crystallinity.